International Food Research Journal 29(5): 1168 - 1178 (October 2022)
Journal homepage: *http://www.ifrj.upm.edu.my*

Sterilising effect of high power pulse microwave on *Listeria monocytogenes*

[1,2]Zhang, Y. X., [2]Wang, F., [2]Wu, H., [2]Fan, L. L., [1,2]Wang, Y., [1,2]*Liu, X. L. and [2]*Zhang, H. Z.

[1]*School of Food and Biological Engineering, Jiangsu University, Zhenjiang 212013, China*
[2]*Institution of Argo-Product Processing, Jiangsu Academy of Agricultural Sciences, Nanjing 210014, China*

Article history

Received:
14 September 2021
Received in revised form:
27 January 2022
Accepted:
14 March 2022

Keywords

high power pulse microwave, Listeria monocytogenes, sterilisation, membrane damage

Abstract

In the present work, *Listeria monocytogenes* was used as the target strain to investigate the sterilising potential and mechanism of high power pulse microwave (HPPM). Results showed that the inactivation was positively correlated with the pulse frequencies and operating times. The count of *Listeria monocytogenes* was decreased by 5.09 log CFU/mL under 200 Hz for 9 min, which was used as the optimised condition to further explore the sterilisation mechanism. Scanning electron microscopy (SEM) and transmission electron microscopy (TEM) images showed that the *L. monocytogenes* cells of untreated group presented intact surfaces, clear boundary, and its intracellular contents distributed uniformly in the cytoplasm. Following treatment, the cell wall surfaces began to deform in small areas, and cell membranes were severely ruptured, thus resulting in the appearance of electron transmission areas. Extracellular protein and nucleic acid contents, represented by $OD_{260\ nm}$ and $OD_{280\ nm}$, increased with the increase in operating time significantly. After treatment, SDS-PAGE profiles of whole-cell proteins displayed that the protein bands became lighter or even disappeared. Na^+ K^+-ATPase activities and intracellular ATP content decreased by 72.97 and 79.09%, respectively. This was consistent with the cell viability of *L. monocytogenes* observed by confocal laser scanning microscopy. Overall, the sterilisation mechanism of HPPM on *L. monocytogenes* may be caused by membrane damage, intracellular component leakage, and energy metabolism hindrance.

DOI
https://doi.org/10.47836/ifrj.29.5.18

Introduction

Listeria monocytogenes is a Gram-positive, rod-shaped bacterium, and recognised as one of the globally widespread life-threatening foodborne pathogens (Qian *et al.*, 2020). This bacterial pathogen causes listeriosis, which is represented by septicaemia, meningitis, miscarriage, and stillbirth, with the highest case fatality rate recorded in the European Union (Cabanes *et al.*, 2002; Kannan *et al.*, 2020; EFSA and ECDC, 2020). *L. monocytogenes* is ubiquitous in nature, and can survive throughout food processing in meat, vegetables, fish, as well as dairy products (Duze *et al.*, 2021). This bacterial pathogen is highly tolerant to stressful conditions including low pH, high salt concentration, and refrigeration temperature (0 - 4°C) (Lebow *et al.*, 2017; Govaert *et al.*, 2018; Boucher *et al.*, 2021). The consumption of contaminated foods causes foodborne illnesses, and an increase in the incidence of foodborne illnesses is a major public health problem (Bogino *et al.*, 2013). To date, it is still a challenge to inactivate *L. monocytogenes* in food products.

Thermal processing is usually used to pasteurise foodborne pathogens in the food industry. However, it may achieve incomplete decontamination, and cause loss of nutrition value, thus becoming a less popular technology (Alves Filho *et al.*, 2020). These limitations in thermal processing are driving the search for new alternatives (Machado-Moreira *et al.*, 2021). Nowadays, non-thermal techniques such as ultra-high pressure (UHP), low temperature plasma (LTP), high intensity pulse magnetic field (PMF), high intensity pulse electric field (PEF), or irradiation can potentially be used as alternatives to the conventional heating (Aronsson *et al.*, 2005; Maktabi *et al.*, 2011). It is, therefore, imperative for the non-thermal processing to have

*Corresponding author.
Email: liuxiaoli@jaas.ac.cn ; zhz0731@sina.cn

similar or higher inactivation efficiency as compared to thermal processing (Gupta and Abu-Ghannam, 2012). The reactive radicals generated by irradiation result in improved food shelf-life, but they can also react with chemical components and generate radiolytic products such as formaldehyde and short chain hydrocarbons (Ravindran and Jaiswal, 2017). The limitation of low temperature plasma processing is mainly the increase in lipid oxidation, thus causing a huge impact on the sensory characteristics of foods (Muhammad *et al.,* 2018). For general consumer, irradiation and low temperature plasma are considered as immature method of food processing (Ravindran and Jaiswal, 2019). Due to the pressure generated by the ultra-high pressure processing, foods and their packaging's are prone to deformation (Delincée, 1998; Ma *et al.*, 2017). Pulse applied with PEF is for a short period (1~100 μs), and without heat generation (Varalakshmi, 2021). PEF cannot be applied to foods that cannot withstand high fields and form bubbles (Gupta and Abu-Ghannam, 2012).

A growing body of literature has recognised the non-thermal effect of pulsed microwave on bacterial systems (Rougier *et al.,* 2014). It has been shown that pulsed microwave directly interacts with specific (polar) molecules, thus causing a variety of bioeffects, which further leads to failure of the intracellular oxidative defence machinery and DNA damage-mediated inactivation of bacterial cells (Kereya *et al.,* 2018; Shaw *et al.,* 2021). High power pulse microwave (HPPM) has been developed as an innovative non-thermal technology which offers many advantages over other processing technology. HPPM can generate short and high frequency pulse microwave, which is one of electromagnetic waves, with frequencies ranging from 300 MHz to 300 GHz. As one of non-thermal physical technologies, HPPM has gained more attention due to the easy handling after decontamination, and better maintenance of food texture and nutrients. HPPM has been extensively studied in military and medical fields, such as the effects of repeated exposure on cancer incidence and biological effects (de Seze *et al.*, 2020). However, the sterilisation mechanism of HPPM is not entirely clear, which is a challenge for future research.

The aim of the present work was, therefore, to investigate the sterilisation mechanism of HPPM on *L. monocytogenes* from ultrastructural morphology, cell membrane permeability, and energy metabolism.

Materials and methods

Strain suspension preparation

Listeria monocytogenes 21532 was supplied by China Center of Industrial Culture Collection (CICC), and preserved as a stock culture in the Food Bioengineering Laboratory, Institute of Farm Product Processing, Jiangsu Academy of Agricultural Sciences. The strain was recovered on Brain Heart Infusion (BHI; Solarbio, China) medium at 37°C for 24 h, and a single colony was collected. Prior to each experiment, the strain was revived twice in 50 mL of BHI by successively culturing at 37°C for 24 h (Bansal *et al.,* 2021). *L. monocytogenes* cells were collected by centrifuging at 3,000 *g* for 10 min at 4°C. The concentration of strain suspension was adjusted to 1×10^8 CFU/mL with BHI medium.

High power pulse microwave equipment

High power pulse microwave equipment was designed and manufactured by Food Bioengineering Laboratory, Jiangsu Academy of Agricultural Sciences and Nanjing Chongdian Co., Ltd. (Crewson *et al.,* 2001; Juengst *et al.,* 2002). It consisted of pulse microwave generator and treatment chamber (Figure 1). The parameters of HPPM equipment were as follows: voltage, 380 V; peak power, 750 kW; pulse voltage, 25 kV; peak frequency, 3 GHz; and pulse duration, 1.5 μs. The alternating current (AC) was firstly converted into direct current (DC) by the converter in the generator. DC current raised the pulse voltage to 25 kV through a transformer. The 3 GHz pulse microwaves, generated by 25 kV of pulse voltage and the magnetron, were imported to the treatment chamber. The pulse frequency of HPPM is the number of pulses per second (Hz) during the treatment, with the next pulse beginning after the current pulse end.

Optimisation of sterilisation parameters

Firstly, 5 mL strain suspension of *L. monocytogenes* samples, added in a 10 mL polytetrafluoroethylene tube, were treated by HPPM. The samples were treated by HPPM under different pulse frequencies (50, 100, 150, 200, and 250 Hz, respectively), and operating times (3, 5, 7, 9, and 11 min, respectively). Three replicates were performed for each treatment condition.

To investigate the sterilisation ability of HPPM on *L. monocytogenes*, plate counting method was

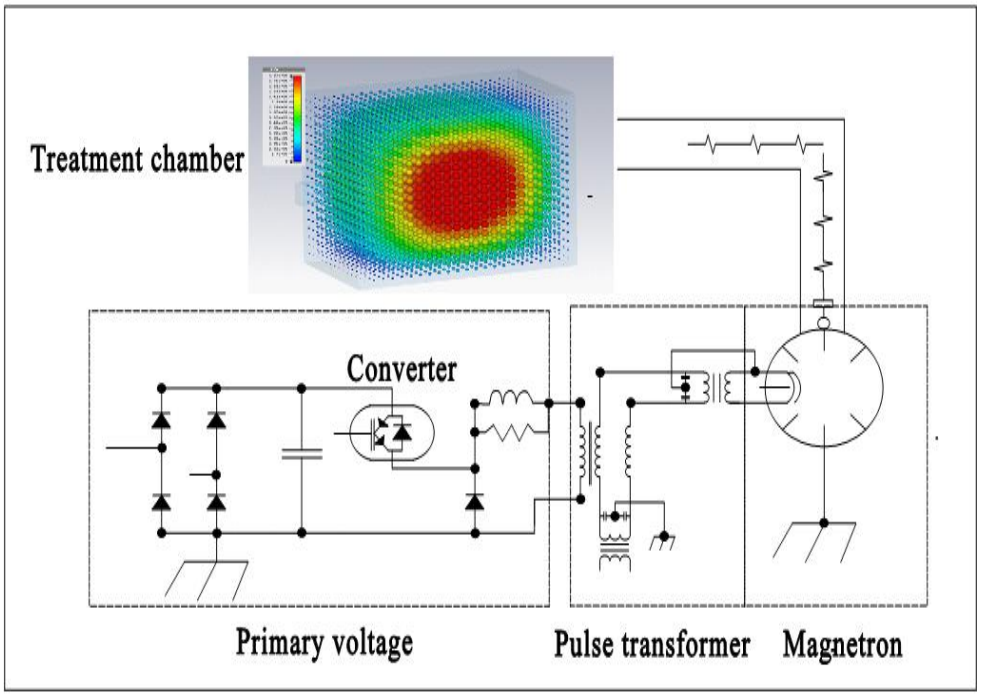

Figure 1. Schematic of high power pulse microwave (HPPM) equipment. Alternating current (AC) was first converted into direct current (DC) by the converter in the generator. DC current then raised the pulse voltage to 25 kV through a transformer. The 3 GHz pulse microwaves, generated by 25 kV of pulse voltage and the magnetron, were then imported to the treatment chamber.

used to determine the number of surviving cells of treated and untreated groups (Xu *et al.*, 2019). Briefly, treated and untreated bacterial suspensions were 10-fold serially diluted in 0.85% (w/v) sterile saline solution. Next, 1 mL of the sample was plated onto BHI agar medium. All of the plates were incubated at 37°C for 24 h. The mortality was expressed as log (N0/N) which indicated the sterilising effect of HPPM treatment. N and N0 are the numbers of surviving cells of HPPM treated and untreated group, respectively (CFU/mL) (Tao *et al.*, 2014).

Scanning electron microscopy (SEM) and transmission electron microscopy (TEM) analyses

Samples of *L. monocytogenes* were centrifuged at 3,000 *g* for 10 min under 4°C to get the pellets. The cells were washed twice with 0.85% sterile saline, and fixed with 2.5% glutaraldehyde solution for 4 h. After washing, *L. monocytogenes* was further fixed with 1% osmium tetroxide (OsO_4) for 2 h, and washed three times with 0.1 M phosphate buffers solution (PBS; pH 7.0). The pellets were dehydrated successively with 30, 50, 70, 80, and 90% ethanol once, and 100% ethanol twice for 15 min. Samples was freeze-dried and sputtered with platinum for 4 min. The morphology of the *L. monocytogenes* cells was observed and photographed with a scanning electron microscope S-3000N (Hitachi, Ltd., Tokyo, Japan) (Fancello *et al.*, 2020). For TEM investigations, the pellets were dehydrated successively, transferred to absolute acetone, embedded in Epon812 epoxy resin for 4 h at 25°C, and polymerised for 24 h in an oven at 65°C. The specimens were sectioned in Leica EM UC7 ultramicrotome (Leica Biosystems, Nussloch, Germany), stained with uranyl acetate and alkaline lead citrate for 5~10 min, and visualised on Hitachi Science and Technology H-7650 transmission electron microscope (Hitachi, Ltd., Tokyo, Japan) (Lv *et al.*, 2018).

Determination of cell membrane permeability and whole-cell protein analysis

The extracellular contents of nucleic acids and proteins of *L. monocytogenes* were detected by measuring the UV absorption at 260 and 280 nm, respectively (Aronsson *et al.*, 2005; Efenberger-Szmechtyk *et al.*, 2021). The absorption peak of the conjugated double bond, existing in tyrosine and tryptophan residues of protein is at 280 nm, and the absorption peak of purines, pyrimidines, nucleosides, and nucleotides in nucleic acids is at 260 nm (Tao *et al.*, 2014). At the same time, the extracellular protein

contents were also determined using a bicinchoninic acid (BCA) protein assay kit (Beyotime Bioengineering Institute, Shanghai, China) (Kang *et al.*, 2020). Briefly, 10 mL of each replicate were centrifuged at 10,000 *g* for 10 min at 4°C. The supernatant was obtained and measured at wavelengths of 280 and 260 nm by spectrophotometer. The measurements were corrected with the absorbance of the 0.85% sterile saline solution.

The whole-cell protein contents were determined using a bicinchoninic acid (BCA) protein assay kit (Beyotime Bioengineering Institute, Shanghai, China), and analysed by sodium dodecyl sulphate-polyacrylamide gel electrophoresis (SDS-PAGE). SDS-PAGE was based on the previous method with some modifications (Kang *et al.*, 2020). The protein samples were mixed with the 5× protein loading dye in a ratio of 1:4. After boiling for 15 min, the mixtures were cooled on ice, and then centrifuged. For whole-cell proteins analysis, electrophoresis was carried out using 5% stacking and 12% resolving gels. The gels were stained with Coomassie brilliant blue R-250, and photographed under the automatic digital gel image analysis system (Tanon-3500R, Shanghai, China).

Determination of ATP content and ATPase activity

Treated and untreated bacterial suspensions were collected by centrifugation (3,000 *g*, 4°C, 10 min), and washed three times with prechilled PBS buffer. The cells were lysed using the lysis buffer associated with the enhanced ATP assay kit, S0027 (Beyotime Biotechnology, Shanghai, China). The ATP content and Na^+ K^+-ATPase activity of *L. monocytogenes* cells was assayed using an enhanced ATP and ATPase assay kit (Jiancheng Bioengineering Institute, Nanjing, China) following the manufacturer's instructions, respectively (Zhou *et al.*, 2016; Lin *et al.*, 2019a). The ATP content and Na^+ K^+-ATPase activity were expressed as nmol/L and U/mgprot, respectively.

Determination of cell viability

The cell viability was determined using a LIVE/DEAD Bacterial Staining Kit (BBcellProbe® N01/PI, BestBio), and observed by confocal laser scanning microscopy (CLSM) (Ren *et al.*, 2020). There were two fluorescent probe stains (N01: excitation wavelength at 488 nm and emission wavelength at 500 nm; PI: excitation wavelength at 561 nm and emission wavelength at 617 nm) in the kit. After centrifugation, the fluorescent probe stains (N01 and PI) were added onto *L. monocytogenes*, and kept at room temperature in the dark for 30 min. Then probe-loaded cells were washed three times with 0.85% saline solution, and photographed under the Ultra ViewVoX spinning-disk confocal microscope (Perkin Elmer, Waltham Mass, USA) (Liu *et al.*, 2020).

Statistical analysis

All experiments were carried out in triplicates, and the results expressed as means ± standard deviations. SPSS 13.0 software (Chicago, IL, USA) was applied for the statistical analysis, and one-way analysis of variance (ANOVA) was used to express the significance of differences ($p < 0.05$).

Results and discussion

Sterilisation activity of HPPM

L. monocytogenes were treated by HPPM for 7 min with the pulse frequencies ranging from 50 to 250 Hz. The mortality of *L. monocytogenes* increased with increasing pulse frequencies of HPPM (Figure 2A). When the frequencies were below 100 Hz, the sterilisation effect was not obvious. With the further increase of pulse frequencies up to 150, 200, and 250 Hz, the mortality was 2.39, 3.27, and 4.30, respectively. When the frequency was 200 Hz, the temperature of the bacterial suspension increased to about 38.6 ± 1.0°C (Fox *et al.*, 2008). Combined with the cumulative effect of HPPM, the temperature of the bacterial suspension increased significantly at 250 Hz with 56.5 ± 1.0°C. To avoid the influence of thermal effect, the pulse frequencies of high power pulse microwave was selected as 200 Hz.

Figure 2B shows the sterilisation effect of different operating time on *L. monocytogenes*. The mortality increased with increasing operating times. When compared with the untreated group, the count of *L. monocytogenes* decreased by 0.59 log CFU/mL when the operating time was 3 min. When the operating time changed from 7 to 9 min, the mortality significantly increased by 1.54 times. When the operating time was 7, 9, and 11 min, the mortality was 3.31, 5.09, and 5.56, respectively. After treatment (200 Hz, 9 min), the temperature increased by 15.8 ± 0.65°C when compared with the initial temperature (25°C). It has been shown that the temperature has no influence in *L. monocytogenes* cells (McKenzie *et al.*,

2014). Considering the energy consumption and thermal effect, the pulse frequencies of 200 Hz and operating time of 9 min were selected to explore the sterilisation mechanism of HPPM on *L. monocytogenes*.

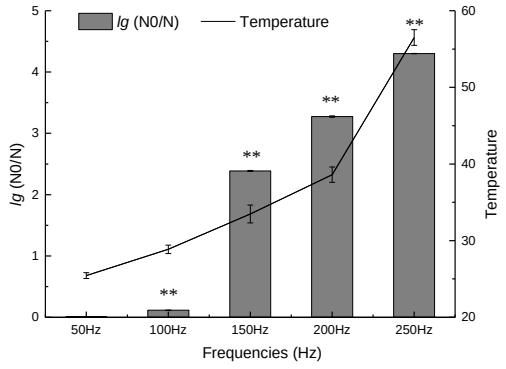

(a)

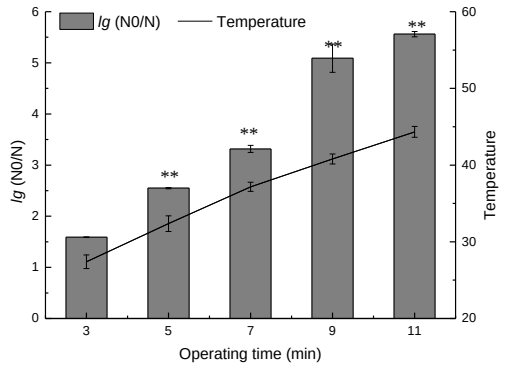

(b)

Figure 2. Sterilisation activity and temperature changes of HPPM treatment with different pulse frequencies **(a)** and operating times **(b)** on *L. monocytogenes.*

Cell morphology observation

Scanning electron microscopy is mainly used to evaluate the morphology of bacteria cells. As shown in Figure 3, the *L. monocytogenes* cells of untreated group presented plump and smooth surfaces, thus indicating vigorous growth. After treatment, the membrane of *L. monocytogenes* experienced depression and roughness. It was inferred that electromagnetic waves affected the morphology of bacteria, thus causing severe morphological changes (Boudjema *et al.*, 2019).

TEM was carried out to directly observe membrane damage and intracellular structural changes induced in *L. monocytogenes* upon exposure to HPPM. The brightness of the image is related to the density of substances that the electrons pass through (Chai *et al.*, 2021). Electrons were scattered by dense objects strongly, shown as dark areas, whereas electrons can pass through thin objects directly, shown as bright areas (electron transmission areas) (Wang *et al.*, 2019). As shown in Figure 4, the *L. monocytogenes* cells of untreated group presented intact surfaces, clear boundary, and their intracellular contents distributed uniformly in the cytoplasm. After treatment, the cell wall surfaces began to deform in small areas, and cell membranes were severely ruptured, thus resulting in the appearance of electron transmission areas. It was inferred that the high energy of HPPM might have damaged the cell membranes, thus leading to the outflow of intracellular components (*e. g.* proteins, nucleic acid) (Yoon *et al.*, 2021). In addition, the dense objects in treated cells were assumed to be condensed DNA and denatured proteins of *L. monocytogenes* (Wang *et al.*, 2015).

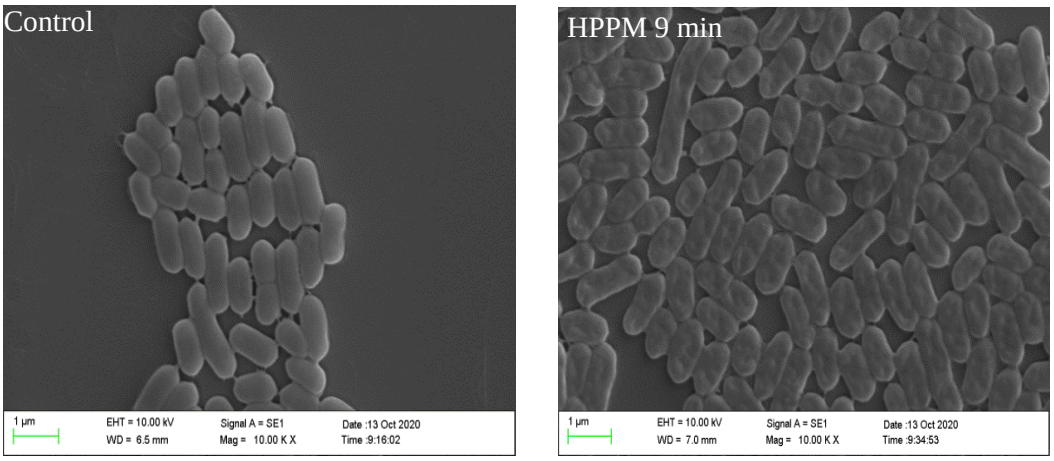

Figure 3. Scanning electron microscopy images of *L. monocytogenes* with HPPM treatment.

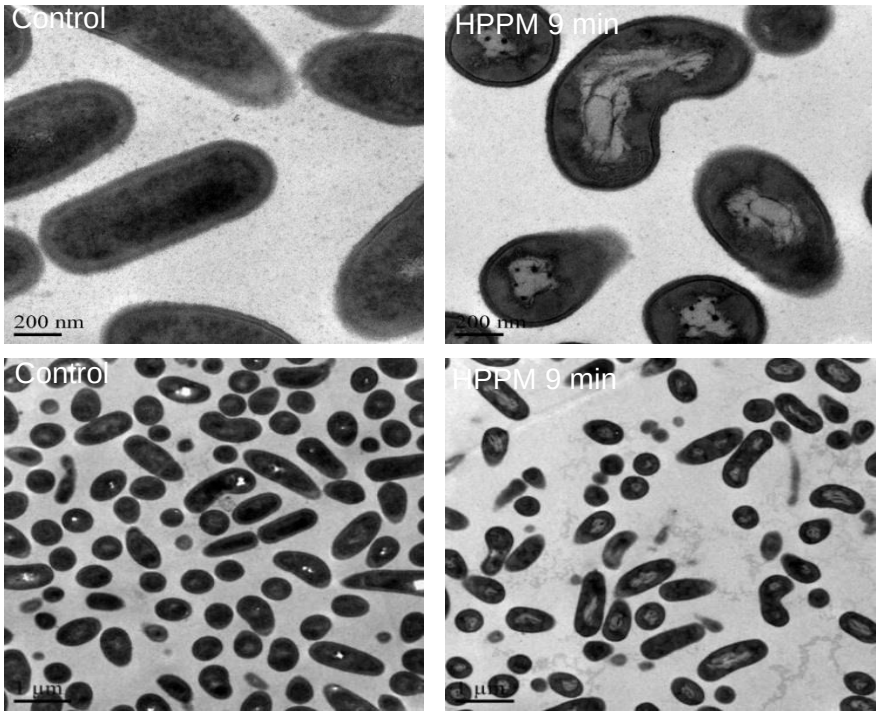

Figure 4. Transmission electron microscopy images of *L. monocytogenes* with HPPM treatment.

Change in cell membrane permeability and whole-cell protein analysis

The leakage of intracellular components can reflect the damage degree of cell membrane (Lin *et al.*, 2019b). As shown in Figure 5A, the absorbance values at 260 and 280 nm gradually increased with increasing operating times. This indicated that HPPM could cause the increase of extracellular protein and nucleic acid contents, as well as the leakage of intracellular components. The absorbance values at 260 nm increased by 1.2, 3.14, 3.34, 3.98, and 4.6 times with 3, 5, 7, 9, and 11 min, respectively. The absorbance values at 280 nm increased by 1.25, 1.75, 2.65, 2.75 and 3.27 times with 3, 5, 7, 9, and 11 min, respectively. Similarly, the soluble protein content under 9 min was 0.081 mg/mL, which was significantly higher than the untreated group (0.025 mg/mL).

As shown in Figure 5B, SDS-PAGE profiles of whole cell proteins displayed the protein bands of untreated *L. monocytogenes* cells with strong intensities. After treatment (200 Hz, 9 min), the protein bands became lighter or even disappeared. This result was consistent with those mentioned earlier, thus indicating that HPPM could change cell membrane permeability and damage the membrane of *L. monocytogenes*, resulting in the leakage of intracellular components.

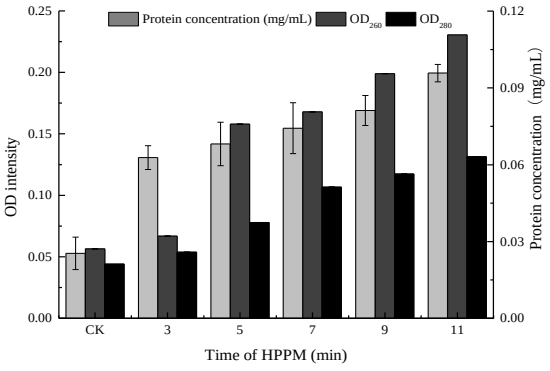

(a)

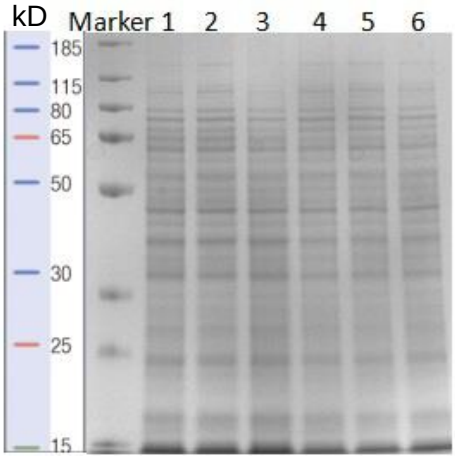

(b)

Figure 5. Extracellular protein and nucleic acid from *L. monocytogenes* cells treated with different operating times **(a)**; and SDS-PAGE profile of intracellular proteins of *L. monocytogenes* cells, the untreated groups are labelled 1, 2, and 3, while the treated groups are labelled 4, 5, and 6 **(b)**.

Change in ATP concentration and ATPase activity

As an important ion channels on the membrane, Na^+ K^+-ATPase play important roles in intercellular signalling, maintaining cell homeostasis, and synthesising ATP (Lin *et al.*, 2019b). ATP participates as a high-energy molecule during many cellular metabolic processes (Filipic *et al.*, 2012). As shown in Figure 6, the intracellular ATP concentration and activities of Na^+ K^+-ATPase of the treated group were 9.634 mmol/L and 0.597 U/mgprot, respectively. When compared with the untreated group, intracellular ATP concentration and activities of Na^+ K^+-ATPase of the treated group decreased significantly by 79.09 and72.97%, respectively ($p < 0.01$). HPPM significantly reduced the intracellular ATP concentration and enzyme activity, which was vital for *L. monocytogenes* growth. It has been reported that electromagnetic wave may lead to the change or denaturation of ATPase, a globular protein whose catalytic activity relies on the native configuration of their active sites and the conformation of surrounding proteins (Ma *et al.*, 2011). The possible reason could be deduced that HPPM promoted the loss of intracellular ATP by causing cell membrane damage and affecting intracellular ATP synthesis or ATPase activity (Kang *et al.*, 2018).

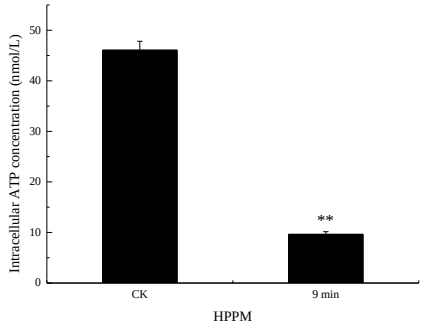

(a)

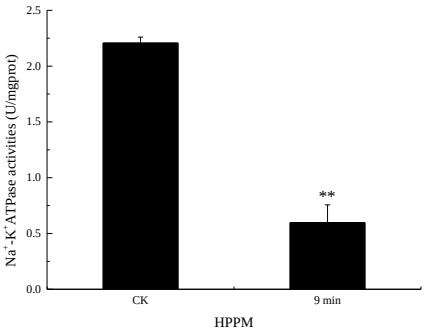

(b)

Figure 6. Effect of HPPM treatment on intracellular ATP concentration **(a)** and activity of Na^+ K^+-ATPase of *L. monocytogenes* **(b)**.

Cell viability

The viability of *L. monocytogenes* cells exposed to HPPM were analysed by CLSM. As shown in Figure 7, the *L. monocytogenes* cells of untreated group showed bright green fluorescence extensively. On the contrary, the *L. monocytogenes* cells of treated group showed sparse green fluorescence, but mainly red fluorescence. The viability of *L. monocytogenes* cells decreased by 8.58%. This result was consistent with those mentioned earlier, thus indicating that HPPM could cause changes in membrane permeability, leading to cell lysis and death.

Conclusion

In the present work, the sterilising effect of high power pulse microwave on *L. monocytogenes* was studied through ultrastructural morphology, cell membrane permeability, and energy metabolism, and the sterilising effect was preliminarily confirmed. Future work could look at DNA damage and changes in virulence gene expression. Considering the energy cumulative effect of HPPM, the sterilisation parameters of pulse frequency and operating time were optimised to 200 Hz for 9 min. The count of *L. monocytogenes* was decreased by 5.09 log CFU/mL under the optimal condition. As shown in SEM and TEM images, untreated *L. monocytogenes* cells had intact surfaces, clear boundary, and the intracellular contents were uniformly distributed in the cytoplasm. Following treatment, the cell wall surfaces began to deform in small areas, and cell membranes severely ruptured, thus resulting in the appearance of electron transmission areas. The high energy of HPPM might have damaged the cell membranes and led to the outflow of intracellular components (*e.g.*, proteins, nucleic acids). The release of intracellular macromolecules was one of the indicators of membrane integrity loss (Efenberger-Szmechtyk *et al.*, 2021). The concentration of extracellular soluble proteins of the treated group was significantly high when compared with the untreated group. Similar trends was also observed from the changes of extracellular protein and nucleic acid contents, which

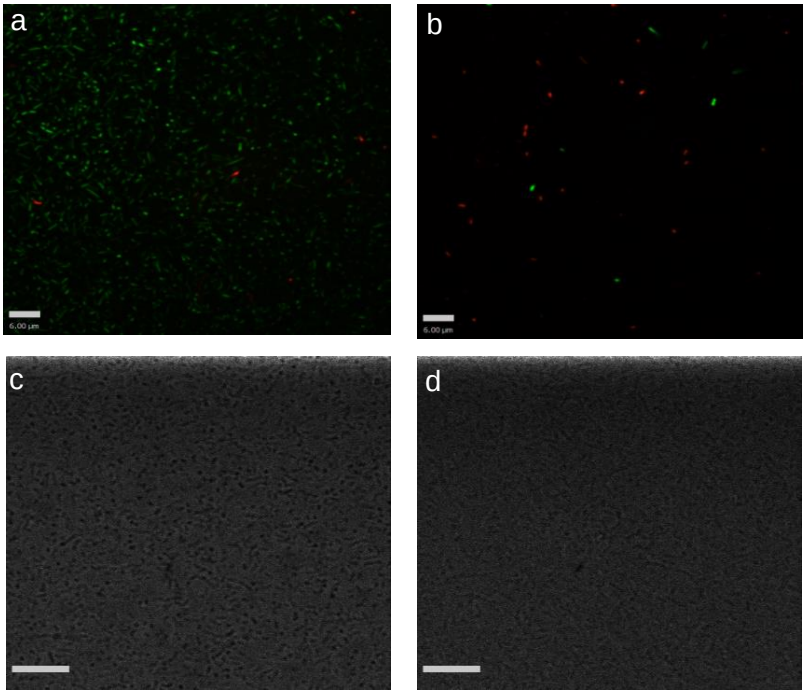

Figure 7. The viability of *L. monocytogenes* cells exposed to HPPM treatment as analysed by CLSM. The cells stained with fluorescent probe N01 are labelled green, while the cells stained with PI are labelled red. The untreated groups are labelled **(a)** and **(c)**, while the treated groups are labelled **(b)** and **(d)**. **(a)** and **(b)** are 2D images in colour mode, while **(c)** and **(d)** are 2D images in grey mode.

were represented by $OD_{260\ nm}$ and $OD_{280\ nm}$. The Na^+ K^+-ATPase activities and intracellular ATP content decreased by 72.97 and 79.09%, thus indicating that the energy metabolism of *L. monocytogenes* was hindered. Based on these results, it can be inferred that HPPM caused changes of membrane permeability and energy metabolism, thus leading to the release of macromolecules, cell lysis, and death.

Acknowledgement

The present work was financially supported by the Jiangsu Agricultural Industry Technology System (grant no.: JATS [2022]448), and Jiangsu Key Research and Development Project (grant no.: BE2019303).

References

Alves Filho, E. G., Silva, L. M. A., Wurlitzer, N. J., Fernandes, F. A. N., Fonteles, T. V., Rodrigues, S. and de Brito, E. S. 2020. An integrated analytical approach based on NMR, LC-MS and GC-MS to evaluate thermal and non-thermal processing of cashew apple juice. Food Chemistry 309: 125761.

Aronsson, K., Rönner, U. and Borch, E. 2005. Inactivation of *Escherichia coli*, *Listeria innocua* and *Saccharomyces cerevisiae* in relation to membrane permeabilization and subsequent leakage of intracellular compounds due to pulsed electric field processing. International Journal of Food Microbiology 99(1): 19-32.

Bansal, M., Dhowlaghar, N., Nannapaneni, R., Kode, D., Chang, S., Sharma, C. S. and Kiess, A. 2021. Decreased biofilm formation by planktonic cells of *Listeria monocytogenes* in the presence of sodium hypochlorite. Food Microbiology 96: 103714.

Bogino, P. C., Oliva, M., Sorroche, F. G. and Giordano, W. 2013. The role of bacterial biofilms and surface components in plant-bacterial associations. International Journal of Molecular Sciences 14(8): 15838-15859.

Boucher, C., Waite-Cusic, J., Stone, D. and Kovacevic, J. 2021. Relative performance of commercial citric acid and quaternary ammonium sanitizers against *Listeria monocytogenes* under conditions relevant to food industry. Food Microbiology 97: 103752.

Boudjema, N., Kherat, M., Drouiche, N. and Mameri, N. 2019. Investigation of the mechanisms of *Escherichia coli* cells sterilization by the application of an electric field. International Journal of Environmental Science and Technology 16(10): 6259-6266.

Cabanes, D., Dehoux, P., Dussurget, O., Frangeul, L. and Cossart, P. 2002. Surface proteins and the pathogenic potential of *Listeria monocytogenes*. Trends in Microbiology 10(5): 238-245.

Chai, Z., Zhang, F., Liu, B., Chen, X. and Meng, X. 2021. Antibacterial mechanism and preservation effect of curcumin-based photodynamic extends the shelf life of fresh-cut pears. LWT - Food Science and Technology 142: 110941.

Crewson, W., Lindholm, M. and Woodburn, D. K. 2001. A new solid state high power pulsed modulator. In the Proceeding of MDK2001 CERN - PS Division, Session 23. Geneva.

de Seze, R., Poutriquet, C., Gamez, C., Maillot-Marechal, E., Robidel, F., Lecomte, A. and Fonta, C. 2020. Repeated exposure to nanosecond high power pulsed microwaves increases cancer incidence in rat. PLoS One 15(4): e0226858.

Delincée, H. 1998. Detection of food treated with ionizing radiation. Trends in Food Science and Technology 9: 73-82.

Duze, S. T., Marimani, M. and Patel, M. 2021. Tolerance of *Listeria monocytogenes* to biocides used in food processing environments. Food Microbiology 97: 103758.

Efenberger-Szmechtyk, M., Nowak, A., Czyzowska, A., Sniadowska, M., Otlewska, A. and Zyzelewicz, D. 2021. Antibacterial mechanisms of *Aronia melanocarpa* (Michx.), *Chaenomeles superba* Lindl. and *Cornus mas* L. leaf extracts. Food Chemistry 350: 129218.

European Food Safety Authority (EFSA) and European Centre for Disease Prevention and Control (ECDC). 2020. The European Union summary report on antimicrobial resistance in zoonotic and indicator bacteria from humans, animals and food in 2017/2018. EFSA Journal 18(3): 6007.

Fancello, F., Petretto, G. L., Marceddu, S., Venditti, T., Pintore, G., Zara, G. and Zara, S. 2020. Antimicrobial activity of gaseous *Citrus limon* var *pompia* leaf essential oil against *Listeria monocytogenes* on *ricotta salata* cheese. Food Microbiology 87: 103386.

Filipic, J., Kraigher, B., Tepus, B., Kokol, V. and Mandic-Mulec, I. 2012. Effects of low-density static magnetic fields on the growth and activities of wastewater bacteria *Escherichia coli* and *Pseudomonas putida*. Bioresource Technology 120: 225-232.

Fox, M. B., Esveld, D. C., Mastwijk, H. and Boom, R. M. 2008. Inactivation of *L. plantarum* in a PEF microreactor. Innovative Food Science and Emerging Technologies 9(1): 101-108.

Govaert, M., Smet, C., Baka, M., Ećimović, B., Walsh, J. L. and Van Impe, J. 2018. Resistance of *L. monocytogenes* and *S.* Typhimurium towards Cold Atmospheric Plasma as function of biofilm age. Applied Sciences 8(12): 2702.

Gupta, S. and Abu-Ghannam, N. 2012. Recent advances in the application of non-thermal methods for the prevention of *Salmonella* in foods. In In Mahmoud, B. (ed). *Salmonella* - A Dangerous Foodborne Pathogen, p. 287-304. United Kingdom: IntechOpen.

Juengst, K.-P., Gehring, R., Kudymow, A., Kuperman, G. and Suess, E. 2002. 25 MW SMES-based power modulator. IEEE Transactions on Applied Superconductivity 12(1): 758-761.

Kang, J., Liu, L., Liu, Y. and Wang, X. 2020. Ferulic acid inactivates *Shigella flexneri* through cell membrane destruction, biofilm retardation, and altered gene expression. Journal of Agricultural and Food Chemistry 68(27): 7121-7131.

Kang, J., Liu, L., Wu, X., Sun, Y. and Liu, Z. 2018. Effect of thyme essential oil against *Bacillus cereus* planktonic growth and biofilm formation. Applied Microbiology and Biotechnology 102(23): 10209-10218.

Kannan, S., Balakrishnan, J. and Govindasamy, A. 2020. *Listeria monocytogenes* - amended understanding of its pathogenesis with a complete picture of its membrane vesicles, quorum sensing, biofilm and invasion. Microbial Pathogenesis 149: 104575.

Kereya, A. V., Zharkova, L. P., Bolshakov, M. A., Kutenkov, O. P. and Rostov, V. V. 2018. Some biological reactions of the organism after exposure to nanosecond repetitive pulsed microwaves. Journal of Physics - Conference Series 1115(2): 022015.

Lebow, N. K., DesRocher, L. D., Younce, F. L., Zhu, M. J., Ross, C. F. and Smith, D. M. 2017. Influence of high-pressure processing at low temperature and nisin on *Listeria innocua* survival and sensory preference of dry-cured cold-smoked salmon. Journal of Food Science 82(12): 2977-2986.

Lin, L., Wang, X. L., He, R. H. and Cui, H. Y. 2019a. Action mechanism of pulsed magnetic field against *E. coli* O157:H7 and its application in vegetable juice. Food Control 95: 150-156.

Lin, L., Wang, X., Li, C. and Cui, H. 2019b. Inactivation mechanism of *E. coli* O157:H7 under ultrasonic sterilization. Ultrasonics Sonochemistry 59: 104751.

Liu, F., Liu, Y., Sun, Z., Wang, D., Wu, H., Du, L. and Wang, D. 2020. Preparation and antibacterial properties of ε-polylysine-containing gelatin/chitosan nanofiber films. International Journal of Biological Macromolecules 164: 3376-3387.

Lv, R., Wang, D., Zou, M., Wang, W., Ma, X., Chen, W. and Liu, D. 2018. Analysis of *Bacillus cereus* cell viability, sublethal injury, and death induced by mild thermal treatment. Journal of Food Safety 39(1): e12581.

Ma, H., Huang, L. and Zhu, C. 2011. The effect of pulsed magnetic field on horseradish peroxidase. Journal of Food Process Engineering 34: 1609-1622.

Ma, L., Zhang, M., Bhandari, B. and Gao, Z. 2017. Recent developments in novel shelf life extension technologies of fresh-cut fruits and vegetables. Trends in Food Science and Technology 64: 23-38.

Machado-Moreira, B., Tiwari, B. K., Richards, K. G., Abram, F. and Burgess, C. M. 2021. Application of plasma activated water for decontamination of alfalfa and mung bean seeds. Food Microbiology 96: 103708.

Maktabi, S., Watson, I. and Parton, R. 2011. Synergistic effect of UV, laser and microwave radiation or conventional heating on *E. coli* and on some spoilage and pathogenic bacteria. Innovative Food Science and Emerging Technologies 12(2): 129-134.

McKenzie, K., Maclean, M., Timoshkin, I. V., MacGregor, S. J. and Anderson, J. G. 2014. Enhanced inactivation of *Escherichia coli* and *Listeria monocytogenes* by exposure to 405 nm light under sub-lethal temperature, salt and acid stress conditions. International Journal of Food Microbiology 170: 91-98.

Muhammad, A. I., Xiang, Q., Liao, X., Liu, D. and Ding, T. 2018. Understanding the impact of nonthermal plasma on food constituents and microstructure—a review. Food and Bioprocess Technology 11(3): 463-486.

Qian, J., Zhang, M., Dai, C., Huo, S. and Ma, H. 2020. Transcriptomic analysis of *Listeria monocytogenes* under pulsed magnetic field treatment. Food Research International 133: 109195.

Ravindran, R. and Jaiswal, A. K. 2017. Toxicological aspects of irradiated foods. In Ferreira, C. F. R., Antonio, A. L. and Verde, S. C. (eds). Food Irradiation Technologies: Concepts, Applications and Outcomes, p. 337-351. United Kingdom: The Royal Society of Chemistry.

Ravindran, R. and Jaiswal, A. K. 2019. Wholesomeness and safety aspects of irradiated foods. Food Chemistry 285: 363-368.

Ren, L., Chen, J., Lu, Q., Wang, C., Han, J., Huang, K. and Wu, H. 2020. Construction of high selectivity and antifouling nanofiltration membrane via incorporating macrocyclic molecules into active layer. Journal of Membrane Science 597: 117641.

Rougier, C., Prorot, A., Chazal, P., Leveque, P. and Leprat, P. 2014. Thermal and nonthermal effects of discontinuous microwave exposure (2.45 gigahertz) on the cell membrane of *Escherichia coli*. Applied and Environmental Microbiology 80(16): 4832-4841.

Shaw, P., Kumar, N., Mumtaz, S., Lim, J. S., Jang, J. H., Kim, D., … and Choi, E. H. 2021. Evaluation of non-thermal effect of microwave radiation and its mode of action in bacterial cell inactivation. Scientific Reports 11(1): 14003.

Tao, X., Chen, J., Li, L., Zhao, L., Zhang, M. and Sun, A. 2014. Influence of pulsed electric field on *Escherichia coli* and *Saccharomyces cerevisiae*. International Journal of Food Properties 18(7): 1416-1427.

Varalakshmi, S. 2021. A review on the application and safety of non-thermal techniques on fresh produce and their products. LWT - Food Science and Technology 149: 111849.

Wang, C. J., Chang, T., Yang, H. and Cui, M. 2015. Antibacterial mechanism of lactic acid on

physiological and morphological properties of *Salmonella* Enteritidis, *Escherichia coli* and *Listeria monocytogenes.* Food Control 47: 231-236.

Wang, H., Zhang, L., Luo, H., Wang, X., Tie, J., Ren, Z. and Kelly, R. M. 2019. Sterilizing processes and mechanisms for treatment of *Escherichia coli* with dielectric-barrier discharge plasma. Applied and Environmental Microbiology 86(1): e01907-19.

Xu, F., Wang, B., Hong, C., Telebielaigen, S., Nsor-Atindana, J., Duan, Y. and Zhong, F. 2019. Optimization of spiral continuous flow-through pulse light sterilization for *Escherichia coli* in red grape juice by response surface methodology. Food Control 105: 8-12.

Yoon, J.-H., Jeong, D.-Y., Lee, S.-B. and Kim, S.-R. 2021. Control of *Listeria monocytogenes* and *Escherichia coli* O157:H7 in enoki mushrooms (*Flammulina velutipes*) by combined treatments with organic acids, nisin, and ultrasound. Food Control 129: 108204.

Zhou, J., Zhang, F., Meng, H., Zhang, Y. and Li, Y. 2016. Introducing extra NADPH consumption ability significantly increases the photosynthetic efficiency and biomass production of cyanobacteria. Metabolic Engineering 38: 217-227.